

CAN202 – Analogue and Digital Communication I

Coursework

Student Name: Yukun.Zheng22

Student ID: 2251625

Submission date: 27/04/2025

ABSTRACT:

Based on MATLAB script coding, this coursework conducts a systematic study on three modulation methods: DSB-SC AM, superheterodyne receiver and FM. The "handel" audio was used to test DSB-SC modulation and coherent detection, a 50 kHz superheterodyne link was constructed to demodulate the target audio, and the FM signal spectrum was analyzed based on different β values. The results reveal the differences among various methods in terms of spectral distribution and signal restoration, providing a reference for modern communication modulation and demodulation processes.

Contents

1. Question 1.....	3
1.1 Part A.....	3
1.2 Part B.....	8
2. Question 2.....	11
3. Question 3.....	16
4. CONCLUSION.....	22

1. Question 1

1.1 Part A

a) Q1_(a)

After executing the "load handel" command in MATLAB, y (audio signal) and the sampling rate $F_s = 8192$ Hz will be imported. By calling instruction "player = audioplayer(y, Fs); play(player)", I can hear the sound of "Hallelujah".

b) Q1_(b)

According to the Nyquist sampling theorem, to avoid aliasing in frequency spectrum, the sampling frequency must be greater than or equal to twice the highest frequency component of the signal. Since the sampling rate provided in this question is 8192 Hz, the maximum frequency range that this audio can safely carry is from 0 to 4096 Hz. In other words, the maximum bandwidth of the modulated signal should be 4096 Hz in turn.

c) Q1_(c)

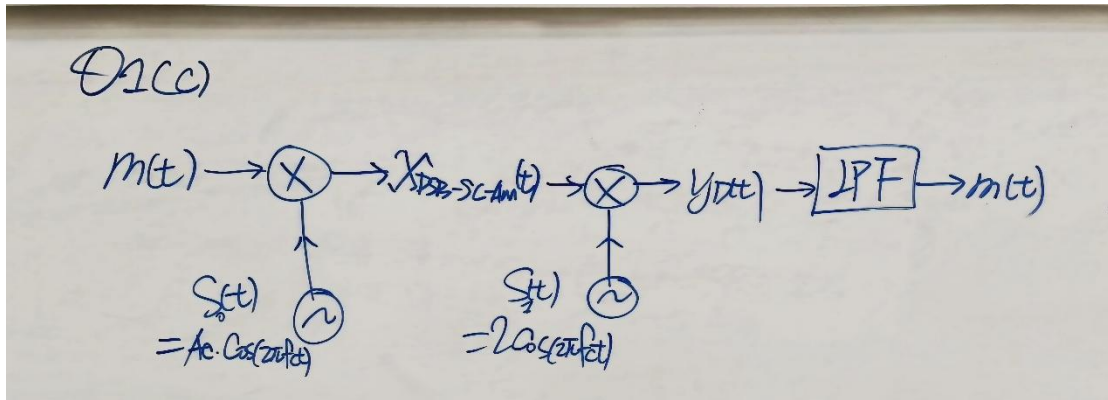


Figure 1: Block Diagram of DSB-SC-AM & Coherent Detection

Figure 1 shows the block diagram of DSB-SC modulation and demodulation.

First, baseband signal $m(t)$ is multiplied by the carrier signal $S_0(t) = A_c * \cos(2\pi * f_c * t)$ to obtain the DSB-SC modulation signal $x_{DSB-SC-AM}(t)$. Then, the modulated signal is demodulated with the carrier again multiply $S_1(t) = 2 * \cos(2\pi * f_c * t)$ to generate the intermediate signal $y_D(t)$ that contains the frequency component of the original message signal. Finally, the high-frequency components are removed through the low-pass filter (LPF) to restore the original message signal $m(t)$. This process fully embodies the modulation and demodulation principles of the DSB-SC signal.

d) Q1_(d)

This figure shows the amplitude spectrum obtained after performing FFT on the loaded Handel audio and applying *fftshift*. The horizontal axis shows the frequency range from $-F_s/2$ to $+F_s/2$. The energy is mainly concentrated in the low-frequency region, reflecting that the main components of the original audio are near the DC. This figure serves as the benchmark for the subsequent signal processing steps. When comparing, the changes and retention of the spectrum during the resampling, modulation and demodulation processes can be intuitively observed.

I have the following graph as:

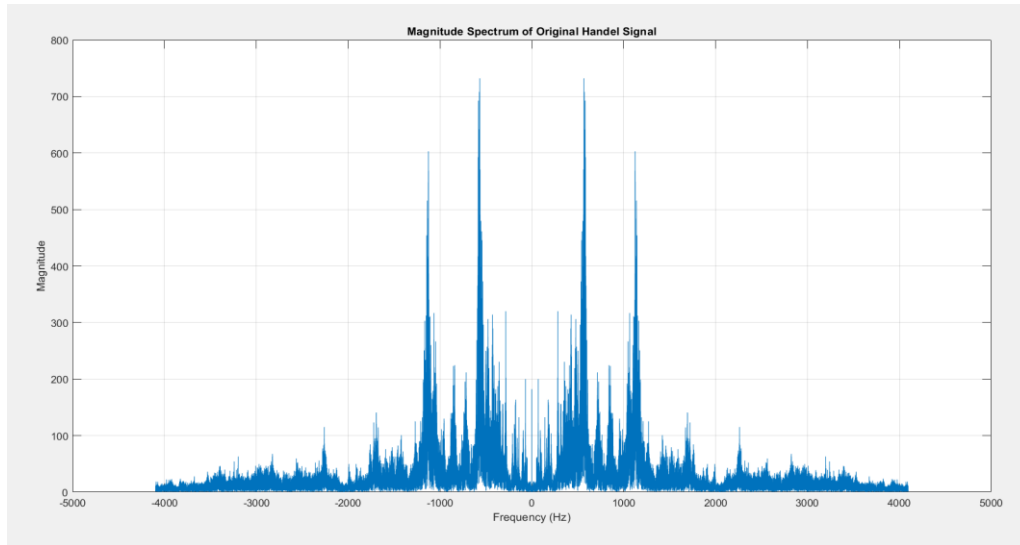


Figure 2: Magnitude Spectrum of Original Handel Signal

e) Q1(e)

According to the Nyquist sampling theorem, in order to avoid frequency aliasing, the sampling frequency must be at least twice the highest frequency component of the signal. In this problem, the original sampling rate of the modulated signal is $F_s = 8192 \text{ Hz}$, and its maximum frequency is approximately $F_s/2 \approx 4096 \text{ Hz}$. According to the requirements of the question, the carrier frequency is set to $f_c = 5 \times 10^5 \text{ Hz}$. Therefore, the frequency range of the modulated DSB-SC signal approximately belongs to $[f_c - 4096, f_c + 4096] \text{ Hz}$.

That is to say, the DSB-SC signal bandwidth is approximately 8192 Hz, and its center frequency is $5 \times 10^5 \text{ Hz}$. To avoid aliasing, the sampling frequency F_{s_new} must be at least twice the frequency range of the modulated signal, namely:

$$F_{s_new} \geq 2 \times (f_c + F_s/2)$$

To satisfy this condition, a calculation formula is given in the question:

$$F_{s_new} = \text{ceil}\left(\left(\frac{F_s}{2} + f_c\right) \times 2\right) \times F_s = 1015808 \text{ Hz}$$

The meaning of this formula is as follows: First, divide the highest frequency component $f_c + F_s/2$ by the original F_s , then multiply it by 2 to obtain a multiple, round it up and multiply it back to F_s , so that F_{s_new} is an integer multiple of F_s . Thus, it can not only avoid aliasing but also facilitate the subsequent interpolation processing of the signal using the 'resample' function.

Therefore, F_{s_new} is a high enough sampling rate and can be used for distortion-free sampling of modulated signals.

f) Q1(f)

In order to perform distortion-free sampling of the modulated signal, I need to increase the sampling rate of the original signal y from $F_s = 8192 \text{ Hz}$ to the calculated $F_{s_new} = 1015808 \text{ Hz}$. This step is called "upsampling". Essentially, it involves inserting more data points between the original sampling points through interpolation, thereby enhancing the

resolution of the signal on the time axis and meeting the requirements of high-frequency carriers during the modulation process.

In MATLAB, I use the 'resample' function to complete this process. This function transforms the signal from the original sampling rate to the target sampling rate in the form of an integer ratio $p:q$. This method not only ensures the accuracy of sampling rate conversion, but also has an anti-aliasing filter built in to prevent the introduction of high-frequency noise during the interpolation process.

Therefore, by sampling y as $y_{upsampled}$, I obtain a high-resolution signal represented under Fs_{new} , providing a good time-domain basis for the subsequent modulation operation.

g) Q1(g)

In order to meet the requirements brought by the carrier frequency being greater than the original audio bandwidth, the audio signal was upsampled, increasing the sampling rate from 8192 Hz to Fs_{new} (approximately 1015808 Hz).

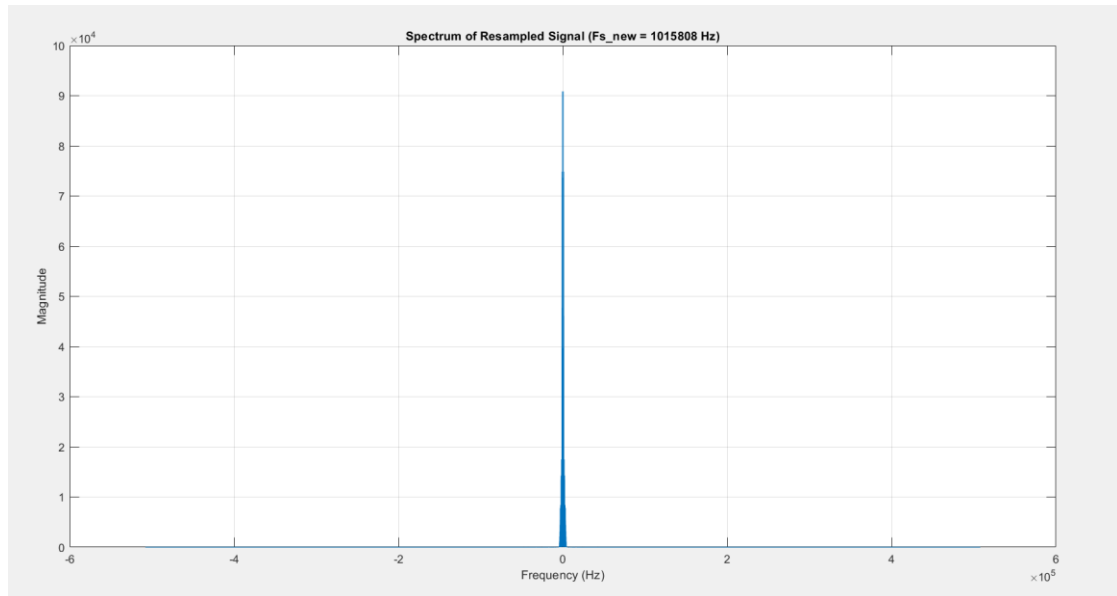


Figure 3: Magnitude Spectrum of Resampled Signal

This figure shows the amplitude spectrum of the resampled signal. Due to the increase in the sampling rate, the spectral range has significantly expanded, but the spectral characteristics of the signal remain essentially consistent. This figure verifies that the spectral aliasing problem has been successfully avoided through resampling and provides a sufficiently high sampling resolution for the subsequent DSB-SC modulation.

h) Q1(h)

In this sub-question, I have to perform a multiplication operation between the upsampled signal $y_{upsampled}$ and a cosine carrier to generate the DSB-SC modulated signal. First, the carrier signal should be

$$fc(t) = \cos(2\pi * fc * t)$$

Where $fc = 5 * 10^5 \text{ Hz}$ as for my student ID number

Second, the sampling frequency is ($F_{s_new} = 1015808 \text{ Hz}$). After that the modulated DSB-SC signal can be obtained by multiplying $y_{\text{upsampled}}$ point by point with the cosine carrier. In this way, the modulation process of DSB-SC was completed, laying the foundation for the subsequent spectrum analysis and demodulation.

i) Q1_(i)

The DSB-SC-AM signal can be plotted in MATLAB, shown as below.

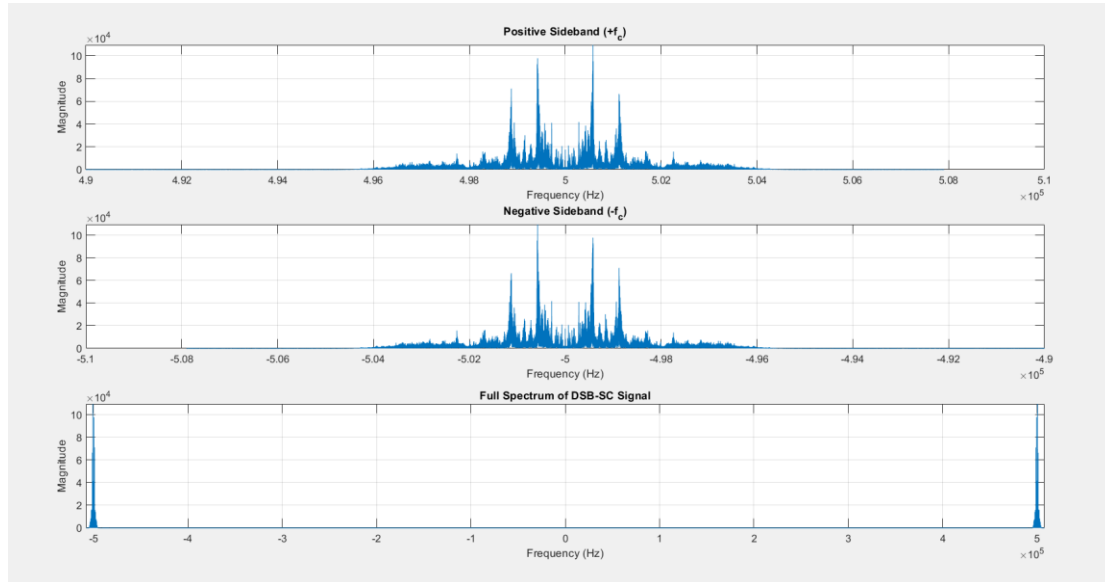


Figure 4: Magnitude Spectrum of DSB-SC Modulated Signal

After DSB-SC modulation, the resampled baseband signal is multiplied by the 500 kHz cosine carrier and multiplied by 2 before the product to perform amplitude compensation, thus forming the modulated signal. As can be seen in Figure 4, the signal spectrum presents a symmetrical distribution of positive and negative sideband bands, with the center located near the positive and negative carrier frequencies, and its bandwidth is consistent with that of the original audio signal. This result indicates that the modulation process is correctly implemented, and the strategy of multiplying by 2 is adopted to effectively compensate for the amplitude attenuation caused during modulation, ensuring that the signal can be completely restored during subsequent demodulation.

j) Q1_(j)

In synchronous demodulation, I multiply the modulated signal again with the carrier signal of the same frequency. This operation shifts the carrier component in the signal and simultaneously generates the DC and $2fc$ components.

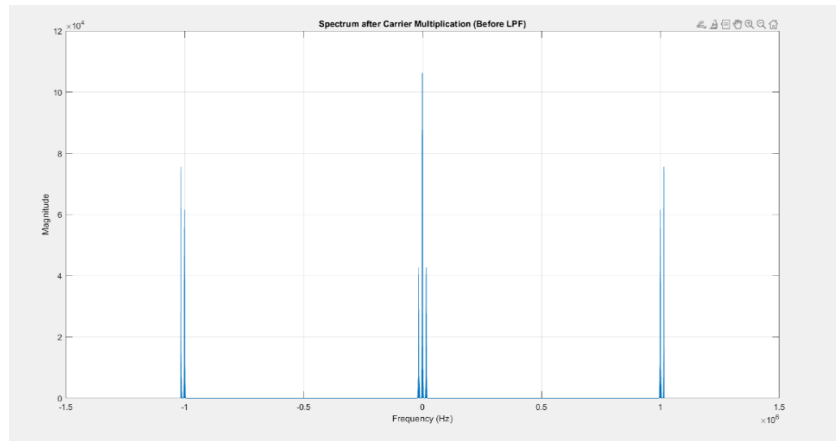


Figure 5: Spectrum after Carrier Multiplication (Before LPF)

This diagram shows the spectral situation multiplied by the carrier (**Note that I multiply the carrier signal by 2 as shown the logic in Q1-c block diagram**). The components near the DC in the spectrum are significantly enhanced, and the components located at the high frequency (approximately $\pm 2f_c$ position) are also clearly visible. This figure indicates that this step successfully completes the frequency conversion under the spectrum, laying the foundation for extracting baseband information through low-pass filtering.

By plotting the spectrum of the product signal, it can be observed that the frequency components are split into two groups. One part is concentrated near the DC, containing the information of the original baseband signal, and the other part is concentrated at the position twice the carrier frequency, which is the unwanted high-frequency component.

k) Q1_(k)

I apply low-pass filtering to the signal that has undergone secondary modulation to extract the baseband signal. During the coherent demodulation process, in addition to the original information contained near the DC, there is also a useless component located at high frequency $2 * f_c$. Therefore, a low-pass filter with a cut-off frequency of 5000 Hz needs to be designed, retaining only the baseband part.

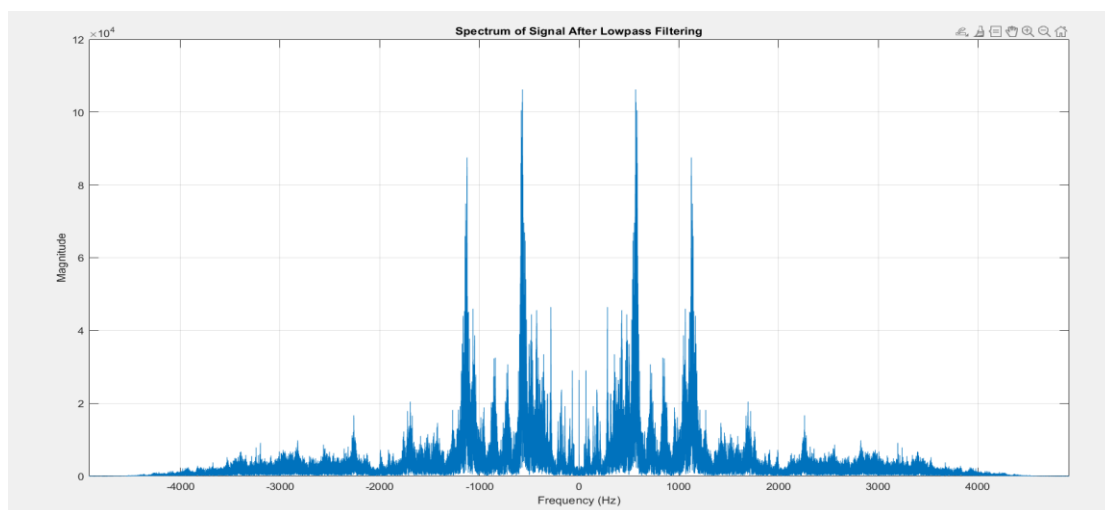


Figure 6: Spectrum after Lowpass Filtering

After being processed by a low-pass filter (with the cut-off frequency set to the Nyquist frequency of the original audio, which is approximately 4096 Hz), the high-frequency spurious components are effectively filtered out and the baseband signal is restored. The spectrum shown in Figure 6 is mainly concentrated in the low-frequency region, which is very similar to the amplitude spectrum of the original Handel signal in Figure 2. This proves that after the DSB-SC modulation and synchronous demodulation process, the original audio signal has been successfully restored. It is particularly worth noting that the design of multiplying by 2 in DSB-SC modulation helps to compensate for amplitude attenuation during demodulation, enabling the restored signal to have a higher spectral matching degree with the original signal and achieving a pure restoration in the auditory perception.

l) Q1_(l)

I downsample the baseband signal restored through low-pass filtering back to the original sampling rate of 8192 Hz in order to be consistent with the original audio signal. By using the *resample* function of MATLAB, the signal was resampled according to a reasonable sampling rate ratio. The downsampled signal was then played. Listening to the audio sound, the restored audio was basically consistent with the initially loaded "handel" track, with a clear and distinguishable melody and good sound quality. This indicates that the entire modulation, demodulation and sampling rate processing process correctly retains the main information of the original signal and achieves high-quality audio restoration.

1.2 Part B

m) Q1_(m)

In part B, I am required to use MATLAB to generate a periodic sawtooth wave signal and extracted its main frequency component through a bandpass filter as a new carrier signal.

Firstly, I generated a sawtooth wave signal with 25 periods using 500 kHz as the carrier frequency. To ensure the fineness of the sawtooth wave shape, a high sampling rate of 20 MHz was selected. The original sawtooth wave shape drawn shows the typical characteristics of linear rise and sudden fall.

Secondly, in order to extract the main carrier components, I designed a bandpass filter with a center frequency of 500 kHz and a bandwidth of 20 kHz to filter the sawtooth wave. The filtered signal (below the figure) shows that the original sawtooth shape has been greatly suppressed, leaving behind an approximate cosine waveform with a smooth amplitude variation centered on 500 kHz .

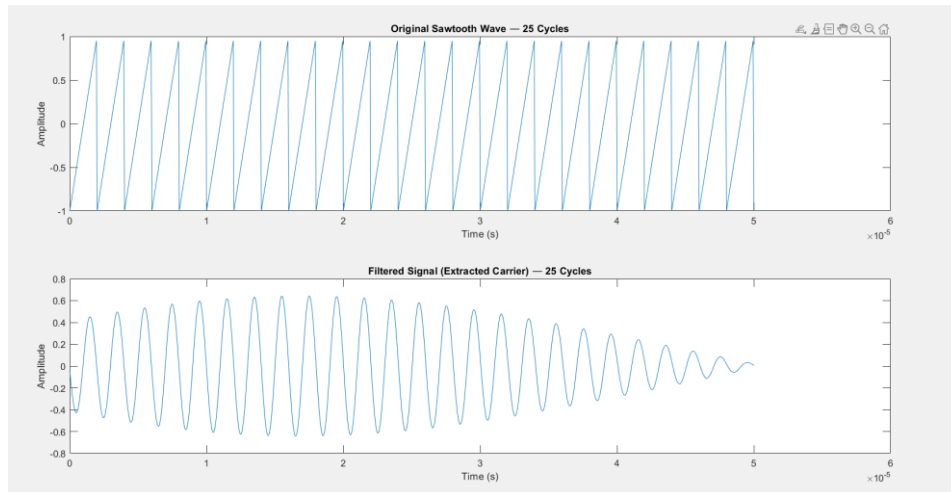


Figure 7: Comparison of Sawtooth Wave Before and After Processing

From the diagram, the main frequency component of the filtered sawtooth wave is significantly prominent, and the time-domain waveform also presents a shape close to a sine wave.

n) Q1_(n)

After completing the extraction of high-quality carriers, the Handel audio samples are modulated as baseband signals.

Firstly, I recalculated the new sampling rate based on the formula to enable it to meet the reasonable separation of the carrier frequency and the baseband signal spectrum.

Secondly, through the resampling operation, the original Handel audio is interpolated to the new sampling rate to ensure that the signal is consistent with the extracted carrier length. To achieve DSB-SC-AM, I multiply the resampled audio signal point by point with the filtered sawtooth carrier to obtain the modulated signal.

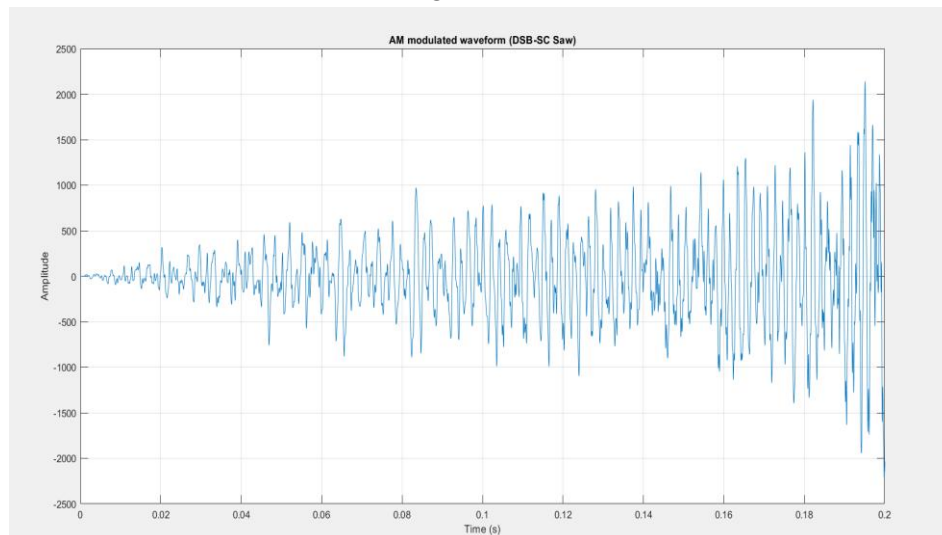


Figure 8: Time Domain of DSB-SC Modulated Signal Using Sawtooth Carrier

It can be observed from the drawn time-domain waveform that the modulated signal as a whole presents the characteristic of rapid oscillation, and its amplitude envelope clearly corresponds to the energy fluctuation of the original Handel audio, verifying the correctness of the modulation process.

o) Q1_(o)

I attempted to demodulate the signal. Specifically, multiply the modulated signal $y_{modulated}(t)$ by the original carrier $carrier(t)$ to obtain a mixed signal containing the DC component and twice the frequency component. Subsequently, a low-pass filter with a cut-off frequency of 5 kHz and an ideal Steepness (Steepness 0.98) effectively filtered out the high frequency interference, retaining only the baseband. The final drawn spectrum diagram shows that the recovered baseband signal spectrum is mainly concentrated within the range of -5 kHz to 5 kHz , and the frequency component distribution is reasonable, verifying the correctness of the harmonic filtering.

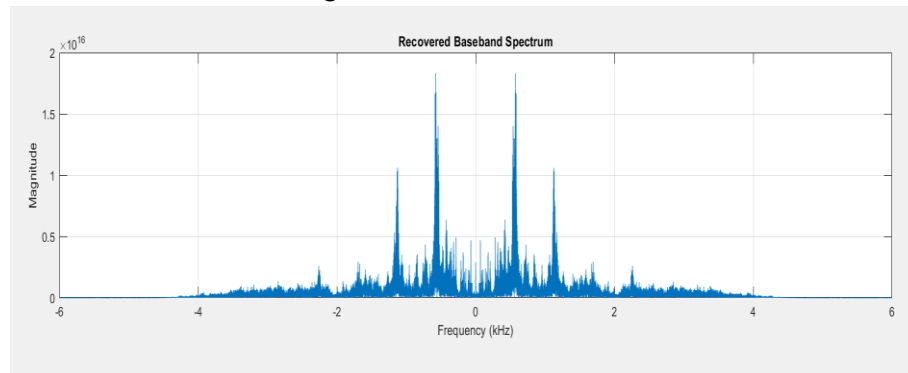


Figure 9: Spectrum of Recovered Baseband Signal After Demodulation

The recovered frequency spectrum indicates both in the time domain and the frequency domain that the demodulation and filtering processes have successfully restored the original audio characteristics.

p) Q1_(p)

In the Q1-p section, I re-downsampled the recovered baseband signal from the high sampling rate to the original audio sampling rate (8192 Hz), and carried out normalization processing to avoid too low volume or distortion. After playing with audioplayer, the sound heard is very pure, without obvious noise or current sound. The sound quality is clear and natural, with only the slight reverberation (hall effect) inherent in Handel music itself. The overall restoration effect is good. It fully demonstrates the effectiveness of the DSB-SC modulation and synchronous demodulation process based on sawtooth wave carrier in this time.

2. Question 2

a) Q2_(a)

I first load the provided composite signal *soundtrack*, whose sampling rate is 1.14 MHz . Subsequently, the *fft* is performed on the signal, and the *fftshift* is used to move the spectral center to the zero-frequency position to facilitate the observation of positive and negative frequency components. To correctly plot the spectrum, the corresponding frequency coordinate axes are constructed, to ensure that the frequency scale matches the actual sampling rate and signal length.

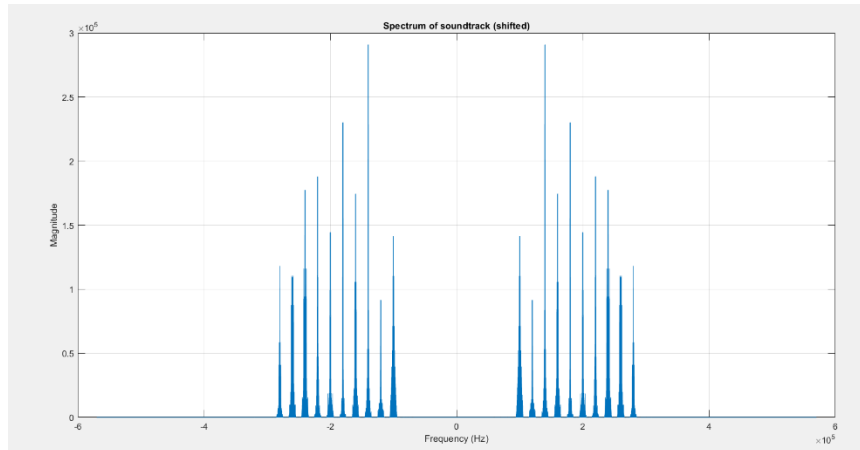


Figure 10: Spectrum of Received Composite Signal

From the drawn spectrum diagram, several communication signals distributed near different carrier frequencies can be clearly seen. Each signal has a limited bandwidth, which is in line with the description in the question that the composite signal contains 10 DSB-SC-AM signals.

b) Q2_(b)

Based on the composite signal spectrum plotted in Q2-a, I observe and identify the 10 modulated signals. The bandwidth of each modulated signal is approximately 10 kHz and is symmetrically distributed around different carrier frequencies respectively. According to the spectrogram, the 10 carrier frequencies can be clearly identified as $1.0 \times 10^5 \text{ Hz}$, $1.2 \times 10^5 \text{ Hz}$, $1.4 \times 10^5 \text{ Hz}$, $1.6 \times 10^5 \text{ Hz}$, $1.8 \times 10^5 \text{ Hz}$, $2.0 \times 10^5 \text{ Hz}$, $2.2 \times 10^5 \text{ Hz}$, $2.4 \times 10^5 \text{ Hz}$, $2.6 \times 10^5 \text{ Hz}$ and $2.8 \times 10^5 \text{ Hz}$ are exactly the same as the requirements of the question. Each signal occupies a frequency band width of approximately 10 kHz , and there is sufficient frequency interval between each signal to avoid mutual interference.

c) Q2_(c)

According to the analysis of Q2-b, the composite signal consists of ten non-overlapping DSB-SC modulation sub-signals, and the bandwidth of each sub-signal is approximately 10 kHz . Since these sub-signals are distributed continuously along the frequency axis without significant overlap, the overall bandwidth is approximately equal to the range from the lowest carrier frequency of $1.0 \times 10^5 \text{ Hz}$ to the highest carrier frequency of $2.8 \times 10^5 \text{ Hz}$, plus the half bandwidth occupied by each signal. It is calculated that the required bandwidth is approximately:

$$\text{Total bandwidth} = (2.8 \times 10^5 + 5 \times 10^3) - (1.0 \times 10^5 - 5 \times 10^3) = 190 \text{ KHz}$$

Among them, 5 kHz is half the bandwidth of each signal. It can be seen from this that in order to completely transmit all the modulated signals in the 'soundtrack', the communication channel requires a bandwidth of at least approximately 190 kHz. This calculation fully takes into account the frequency spread of each signal and is consistent with the spectral observation results.

d) Q2_(d)

The overall structure of the superheterodyne receiver can be described through the following block diagram.

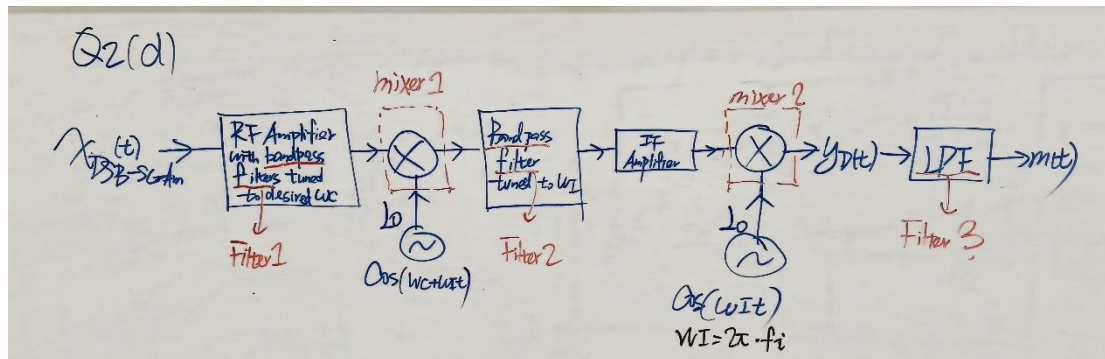


Figure 11: Block Diagram of Superheterodyne Mechanism

Firstly, the received composite signal passes through a radio frequency (RF) bandpass filter, which filters out all frequency components except the target carrier frequency, retaining only the modulated signal of interest.

Then, the signal enters the first mixer (Mixer1) to undergo frequency conversion with the local oscillator (LO) signal, converting the carrier frequency down to the intermediate frequency (IF) frequency.

After frequency conversion, the signal passes through an intermediate frequency bandpass filter to further remove other irrelevant frequency components generated during the mixing process, and only retains the target signal centered on the intermediate frequency.

Next, the signal enters the second mixer (Mixer2), where it is mixed again with a local oscillator signal with a frequency equal to the intermediate frequency, and the signal is eventually transformed to the Baseband.

Finally, through the baseband low-pass filter, the high-frequency noise is filtered out and only the original audio information output is retained, thereby achieving the successful demodulation of the target signal. The entire receiving process involves three filters (RF filter, intermediate frequency filter, baseband filter) and two mixers (RF to IF conversion, intermediate frequency to baseband conversion), and by reasonably selecting the local oscillator frequency to ensure that the intermediate frequency remains constant, the stability and anti-interference ability of the system are enhanced.

e) Q2_(e)

Note that since the analysis have been carried out in Q2-d, therefore, in this section, I focus on the discussion of the results.

- Step 1: Filter1: RF front-end bandpass filter

In the first step, I use a bandpass filter (Filter1) to preprocess the original signal and extract the target frequency band with a center frequency of 200 kHz and a bandwidth of 10 kHz. The filter adopts an 800-order FIR design, ensuring extremely high selectivity and suppression performance. After filtering, the spectrogram shows that only the signal energy is retained near ± 200 kHz, while other frequency components are effectively suppressed, indicating that the filter successfully isolates the part of the signal that needs to be processed, laying the foundation for the subsequent mixing operation.

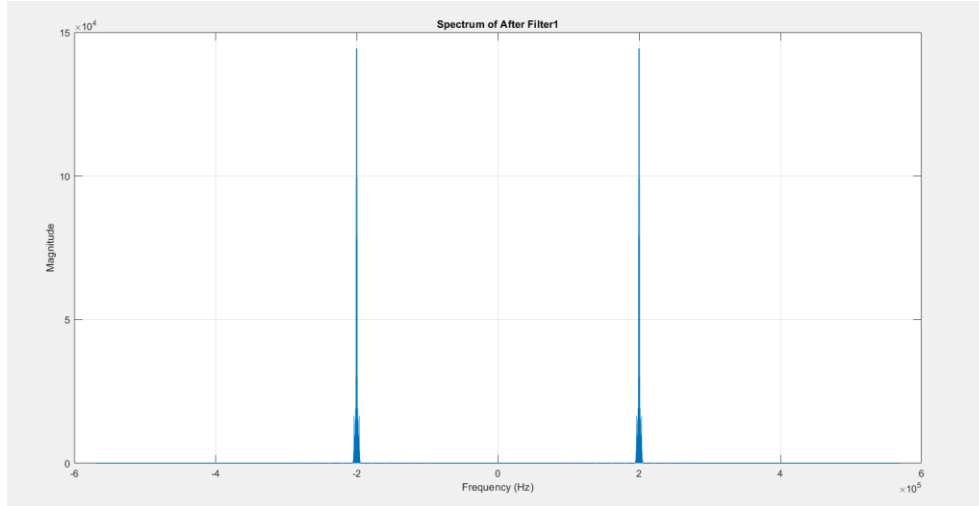


Figure 12: Spectrum after Filter1 (RF Front-End Bandpass Filter)

● Step 2: Mixer1: Downconvert to IF

In the second step, I carried out the first mixing (Mixer1), downconversion the signal from the high-frequency band to the intermediate frequency (IF). To ensure the sampling consistency after mixing, I first perform a minor resampling adjustment on the filtered signal. Then the signal is multiplied by the local oscillator signal with a frequency of $(f_c + f_i) = 250$ kHz, and the spectrum achieves the translation of the center frequency. The spectrogram verified this point, showing that the main spectral components appeared at positions such as ± 50 kHz and ± 450 kHz, which was in line with the expected frequency shift effect.

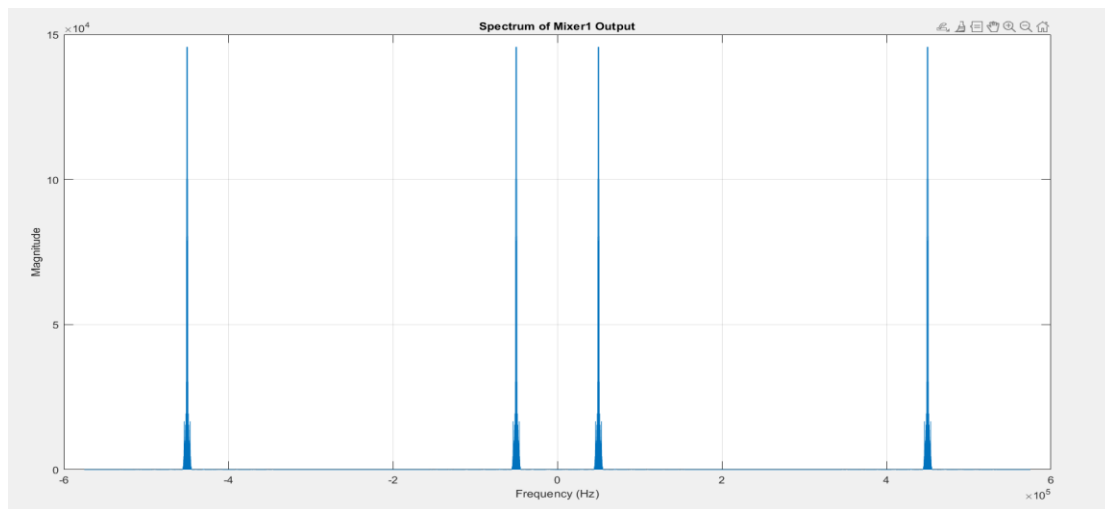


Figure 13: Spectrum after Mixer1 (First Mixing Stage)

● Step 3: Filter2: IF-stage bandpass filter

In the third step, I applied the IF bandpass filter (Filter2) to further filter out the image frequencies and spurious components generated during the mixing process. The center frequency of the filter is set at 50 kHz, and the bandwidth remains at 10 kHz. It can be observed in the spectrum diagram that after filtering, only the effective signal in the mid-frequency band (near ± 50 kHz) is retained, and other frequency components are effectively suppressed. This indicates that the filter plays an important role in cleaning the spectrum and simultaneously improves the signal-to-noise ratio of the system.

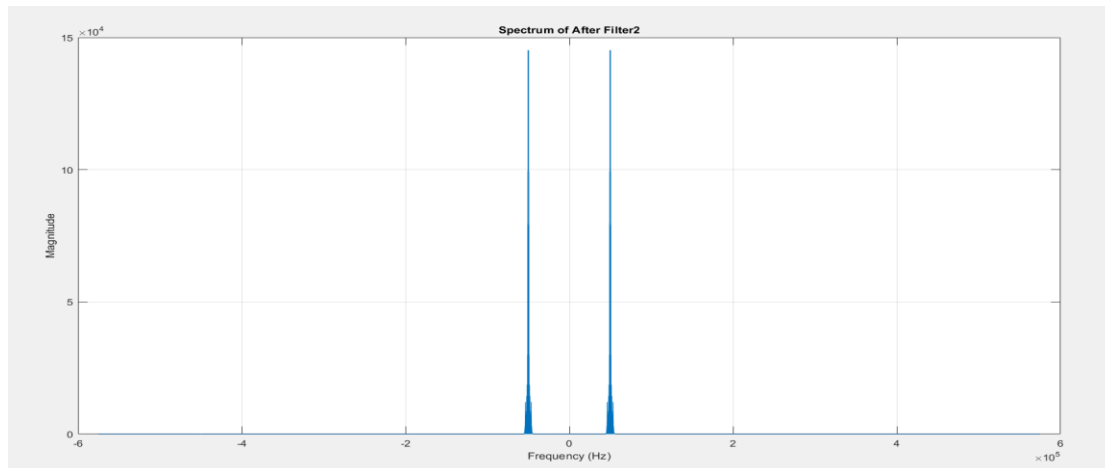


Figure 14: Spectrum after Filter2 (Intermediate Frequency Bandpass Filter)

● Step 4: Mixer2: Downconvert to baseband

In the fourth step, the second mixing (Mixer2) was carried out, that is, the intermediate frequency signal was multiplied by the 50 kHz local oscillator signal again to complete the down-conversion to the Baseband (Baseband) operation. The spectrogram shows that the main energy of the signal has been concentrated near the DC (at 0 Hz), and at the same time, there are residual components around ± 100 kHz. These are secondary frequency components generated after secondary mixing, which conform to the spectral symmetry characteristics. Through this process, the originally high-frequency modulated signal is effectively moved to the low-frequency region, facilitating subsequent processing.

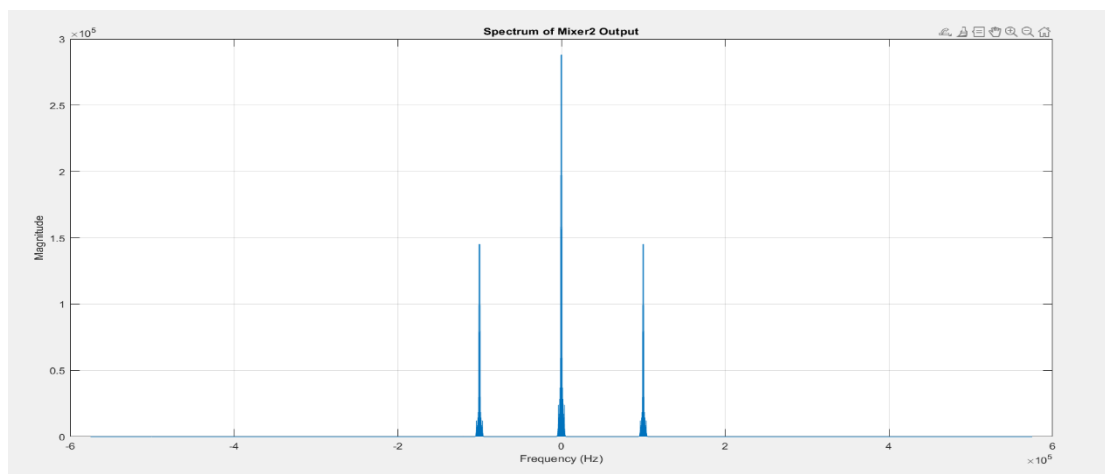


Figure 15: Spectrum after Mixer2 (Second Mixing Stage)

● Step 5: Filter3: Baseband lowpass filter

In the fifth step, I use the baseband low-pass filter (Filter3) to complete the final signal extraction. The cut-off frequency of the filter is 5 kHz, which can retain the main energy of the baseband while suppressing the high-frequency noise residual in the mixing. The spectrogram clearly shows that after filtering, only the narrowband energy distribution is retained near 0 Hz, and the signal purity is significantly improved. Finally, the signal was resampled to the standard audio sampling rate of 10 kHz and normalized for processing, achieving smooth and distortion-free audio reconstruction. The playback effect was good, fully verifying the correctness and effectiveness of the entire high-quality superheterodyne receiver link design.

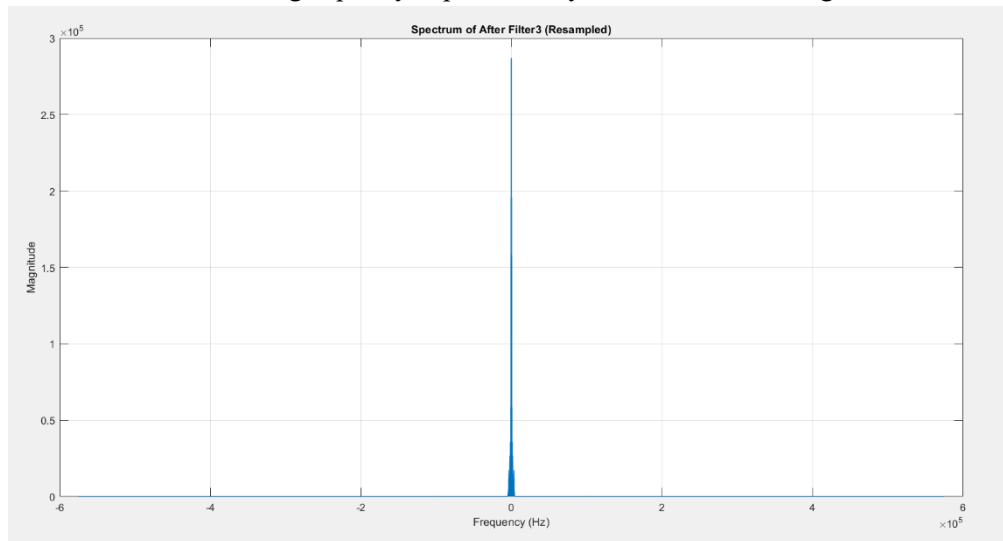


Figure 16: Spectrum after Filter3 (Baseband Lowpass Filter)

● Step 6: Summary

Finally, when the processed audio is played, the melody can be heard clearly and distinguishable, further verifying the correctness and completeness of the tuning process.

f) Q2_(f)

I compared the audio demodulated by the superheterodyne receiver with the ten original audio files provided in music.zip one by one. By listening, it was found that the played audio was completely consistent with the audio of file number 003 in terms of melody, rhythm and timbre, with no obvious distortion or defect. It was confirmed that the tuning process successfully restored the original musical content. This also indicates that no key information was lost in the processing steps such as channel selection, mixing and filtering. The overall system performance is good and has a strong signal fidelity.

g) Q2_(f)

According to the fact that my student number ends with 5, the problem requires the demodulation of a sub-signal with a center frequency of $2.0 \times 10^5 \text{ Hz}$. Through demodulation and comparison, it was found that the audio content obtained by demodulation was completely consistent with the 003.mat file. Therefore, the correct audio file number matched for this question is 003, verifying the system's ability to accurately capture and restore the target sub-signal.

3. Question 3

a) Q3_(a)

According to the requirements of the question, my ID last digit was 5, which selected the modulation index $\beta = 3$ and calculated the values of the first type of Bezier function $J_n(\beta)$ corresponding to different orders $n = 0$ to 5. These Bezier function coefficients represent the amplitude lights of each frequency component in the frequency modulation signal spectrum and are of great significance for analyzing the spectral structure of FM signals. The calculation results show that as the order n increases, the value of the Bezier function gradually decreases, reflecting that the energy contribution of the high-order sideband in the spectrum gradually lakens.

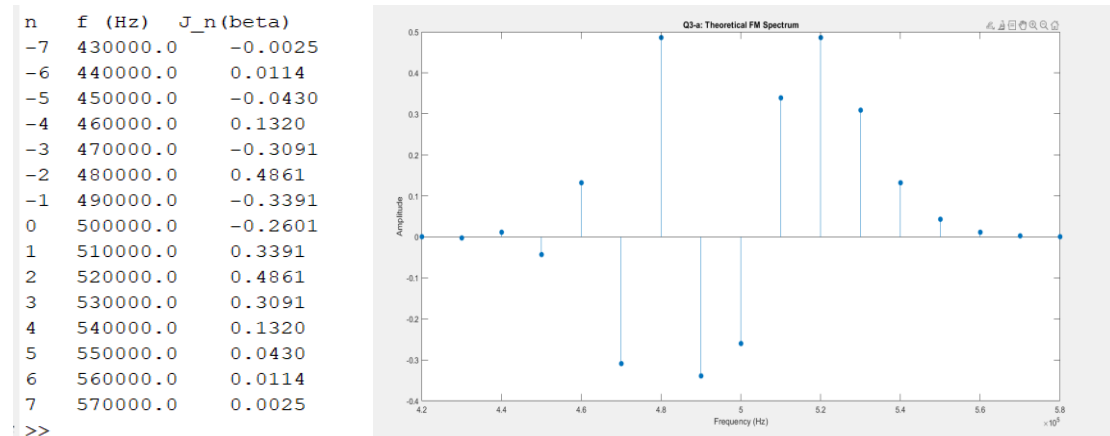


Figure 17: Theoretical FM Spectrum ($\beta=3$)

This is consistent with the theory that the energy of the frequency modulation signal is mainly concentrated in the carrier frequency and several low-order sideband bands nearby.

b) Q3_(b)

In this sub-question, under the condition of a sampling frequency of 10 MHz, I generated a frequency modulation signal $x_{FM}(t)$ with a duration of 0.0003 seconds. The carrier frequency of this signal is set to 500 kHz, the modulated signal frequency is 10 kHz, and the modulation index β is taken as 3. It can be observed from the drawn time-domain waveform diagram that the signal as a whole shows a trend of high-speed oscillation, and in the local area, the compression and expansion phenomena of the waveform alternate.

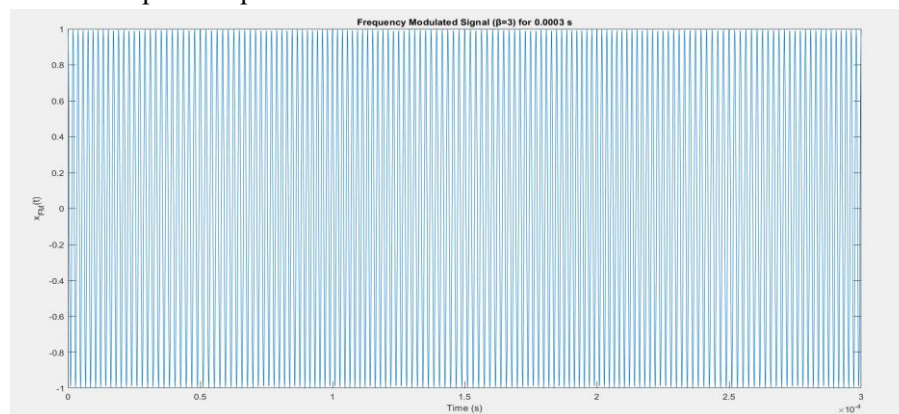


Figure 18: Time Domain of FM Signal ($\beta=3$)

This phenomenon reflects the variation of the signal frequency over time. That is, according to the sinusoidal variation law of the modulated signal, the frequency periodically increases and decreases, which conforms to the typical characteristics of FM signals. Especially in the figure, it can be clearly seen that the signal becomes denser with increased frequency in some time periods and sparse with decreased frequency in others, which intuitively demonstrates the core concept of FM modulation.

c) Q3_(c)

I performed the *fft* on the generated frequency modulation signal $x_{FM}(t)$ and plotted its spectral graph. It can be clearly observed from the figure that the main frequency components of the signal are concentrated at multiple frequency positions centered on the carrier frequency $f_c = 5 * 10^5 \text{ Hz}$. and spaced out at intervals of the modulated signal frequency $f_m = 10^4 \text{ Hz}$. Specifically, the main frequency is located at 500 kHz , and at the same time, multiple groups of sideband components appear on both sides at intervals of 10 kHz .

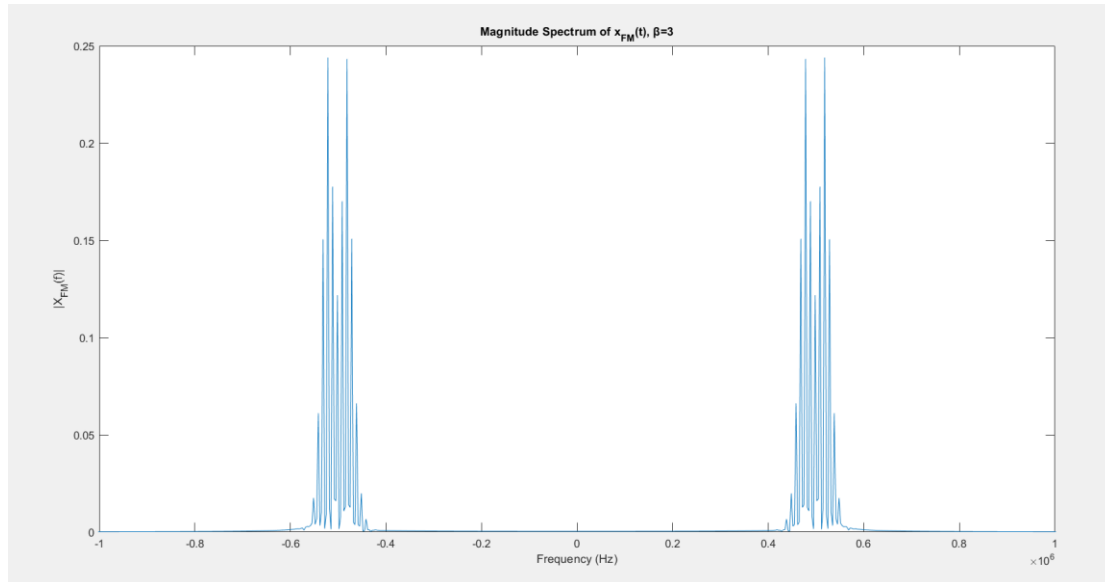


Figure 19: Magnitude Spectrum of FM Signal ($\beta=3$)

This phenomenon is highly consistent with the theoretical derivation of the FM spectral characteristics. The amplitude of each sideband is related to the Bessel function value of the corresponding order. Among them, the energy of the low-order sideband is stronger, and the energy of the high-order sideband decays rapidly. Moreover, the entire spectral distribution is symmetrical and the structure is clear.

d) Q3_(d)

I compared the numerical spectrum results of the frequency modulation signal $x_{FM}(t)$ with the theoretical calculation results. The main frequency components identified in the numerical spectrum are located approximately $\pm 521 \text{ kHz}$, $\pm 481 \text{ kHz}$ and $\pm 478 \text{ kHz}$, $\pm 518 \text{ kHz}$ respectively. It is very close to the position of $f = f_c + n * f_m$ (where n is an integer) calculated theoretically based on the carrier frequency $f_c = 500 \text{ kHz}$ and the modulation frequency $f_m = 10 \text{ kHz}$.

```

>> Q3_2251625
Top 5 numerical spectral lines:
f=-521493 Hz, |X|=0.2439
f=518161 Hz, |X|=0.2439
f=-481506 Hz, |X|=0.2433
f=478174 Hz, |X|=0.2433
f=-511496 Hz, |X|=0.1776
Theoretical spectral components:
Theoretical: f = 480000 Hz, J_-2(β)=0.4861
Theoretical: f = 490000 Hz, J_-1(β)=-0.3391
Theoretical: f = 500000 Hz, J_0(β)=-0.2601
Theoretical: f = 510000 Hz, J_1(β)=0.3391
Theoretical: f = 520000 Hz, J_2(β)=0.4861
>>

```

Figure 20: Spectrum Peak Verification: Numerical vs Theoretical Comparison

Meanwhile, the calculated values of Bessel functions of different orders $J_n(\beta)$ also reflect the amplitude ratios of each sideband and are consistent with the energy magnitude trends of each frequency component in the spectrum. Although there are some slight differences between the numerical frequency and the theoretical frequency due to discrete sampling and limited spectral resolution, the overall result is acceptable.

e) Q3_(e)

I performed a time differential operation on the frequency-modulated signal $x_{FM}(t)$ and further extracted the envelope characteristics of the differential signal.

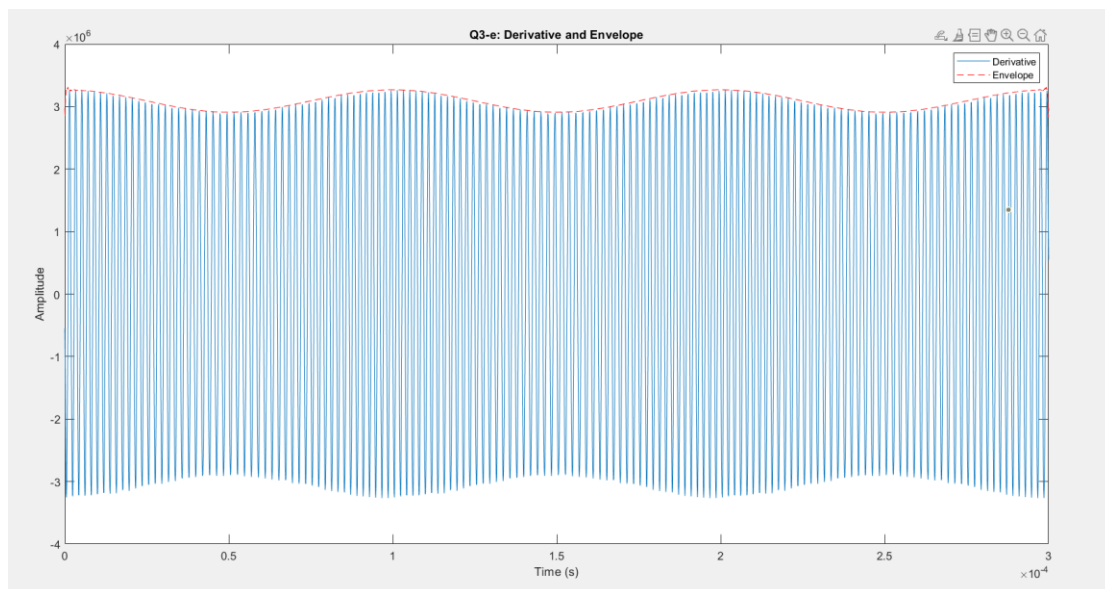


Figure 21: Time Domain of Derivative and Envelope of FM Signal

In this sub-problem, I first performed the derivative operation on the frequency-modulated signal $x_{FM}(t)$ to obtain its differential signal. Since the instantaneous frequency of the frequency modulated signal is proportional to the instantaneous phase derivative of the signal, the differential operation can effectively highlight the frequency variation characteristics. Subsequently, I extracted the envelope of the differential signal by using the Hilbert Transform.

Theoretically, the envelope amplitude of the differentiated frequency modulation signal should be closely related to the amplitude variation of the modulated signal. By observing the drawn image, it can be found that the differential signal shows the characteristic of high-frequency oscillation on the time axis, while the superimposed drawn envelope curve exhibits periodic and slow fluctuations. This changing trend is consistent with the periodic characteristics of the modulation frequency $f_m = 10\text{kHz}$. The overall results verify that the differential and envelope extraction operations can effectively capture the frequency variation information of the frequency modulation signal, providing a theoretical basis for the subsequent demodulation processing.

f) Q3_(f)

I applied ± 0.1 Hard Limiter processing to the original frequency modulation signal $x_{FM}(t)$, and compared the waveform changes of the original signal and the limited signal in the time domain.

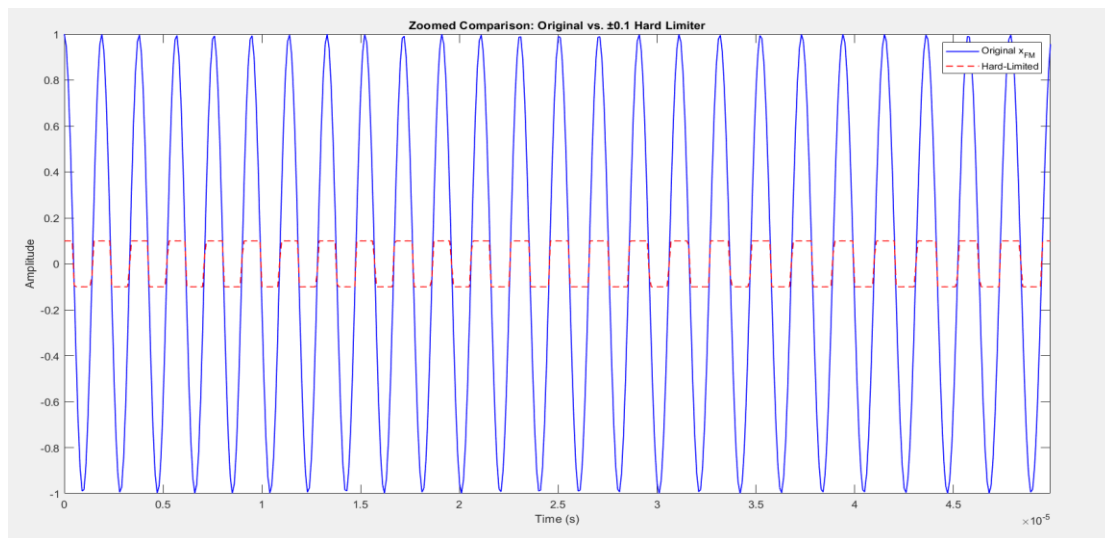


Figure 22: Time Domain Comparison: Original vs Hard-Limited Signal

It can be clearly seen from the comparison graph that **the original signal (the blue curve)** has a continuously changing sinusoidal shape, while the signal processed by the **hard limiter (the red dotted line)** shows a distinct top clipping phenomenon when the amplitude reaches ± 0.1 , forming a shape close to a rectangular wave. It can be further observed through the locally amplified time period that the function of the hard limiter enables the signal to frequently switch amplitude extremes within a very short time, retaining the phase change characteristics in the frequency modulation information, but the amplitude change is forcibly limited. This processing method simulates the limiter function commonly used in actual FM receivers. It can effectively suppress the influence of amplitude noise while keeping the frequency information unchanged and improve the anti-interference ability of the system.

g) Q3_(g)

I conducted a spectral analysis on the signal processed by the hard limiter.

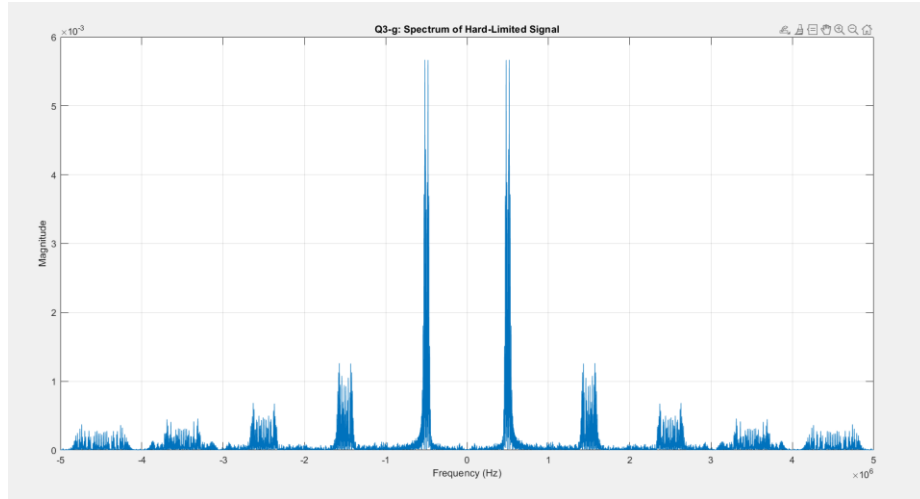


Figure 23: Magnitude Spectrum of Hard-Limited FM Signal

In this sub-question, I conducted a spectral analysis on the frequency modulation signal after processing with a ± 0.1 Limiter limit (Hard Limiter). Through zero-phase limiting, the originally continuously changing frequency modulation signal is forcibly confined within a narrow amplitude range, thereby introducing obvious high-frequency components. By observing the drawn spectrum diagram, it can be found that in addition to the original carrier frequency cluster near $f_c = 500\text{kHz}$, a large number of harmonic components distributed in the higher frequency region also emerged. This is because the limiting operation introduces nonlinear distortion, causing the signal to generate new frequency components. Meanwhile, it can be noted that the signal still has a certain energy distribution near positions such as $\pm 1\text{MHz}$ and $\pm 2\text{MHz}$, which is in line with the theoretical expectation of the generation of high-order harmonics by frequency domain folding and distortion.

h) Q3_(h)

I applied a bandpass filter to the signal after hard limiting processing to remove the high-frequency spurious components generated by limiting and verified the quality of the filtered signal.

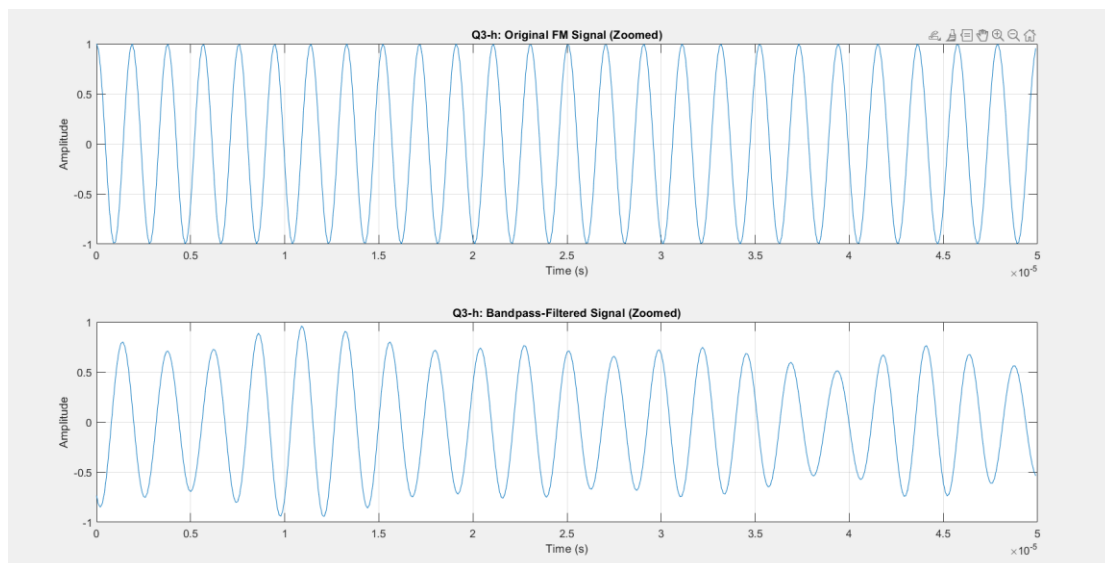


Figure 24: Time Domain Comparison After Bandpass Filtering

Firstly, it can be seen that the original signal retains the complete frequency modulation characteristics in Figure 24. However, after bandpass filtering, the high-frequency noise components of the signal are significantly weakened, and only the main carrier frequency and the effective frequency components near it are retained. Especially within the time range of $t = 0$ to $50 \mu s$, the waveform after bandpass is smoother and the amplitude is reduced. This reflects the effective suppression of non-target frequency components by the filter, while also retaining the main information structure of the modulated signal.

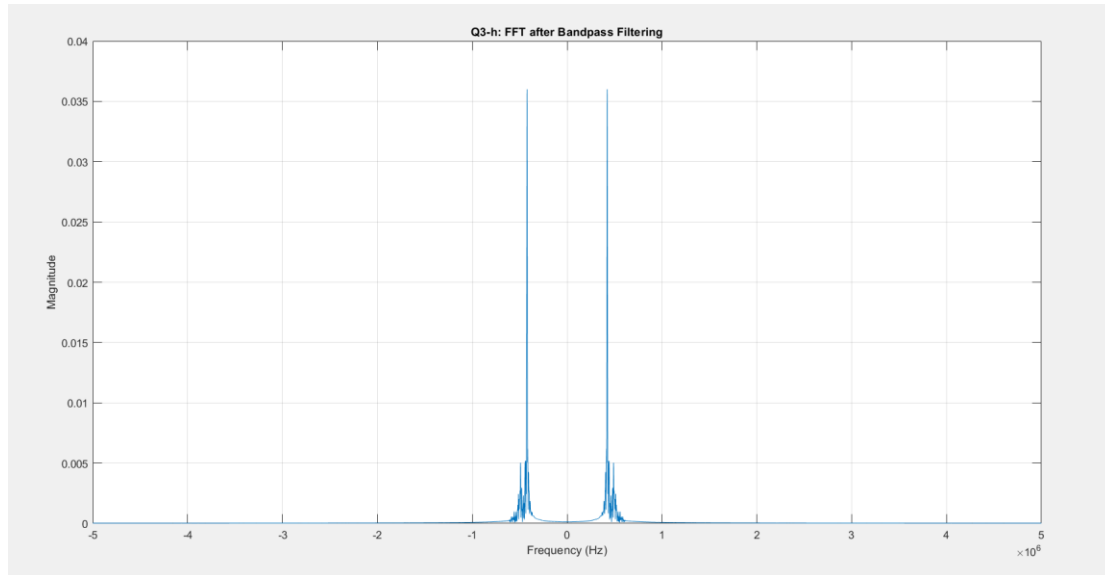


Figure 25: Spectrum After Bandpass Filtering

Secondly, by observing the filtered signal, the signal after bandpass filtering (as shown in the Figure 25) exhibits a clear double main lobe structure, with the center located near $\pm 500 kHz$, which is in line with theoretical expectations. Compared with the hard-limiting signal spectrum (Figure 23) before filtering, it can be clearly observed that the side lobes, which means the stray components far from the main frequency part, have been greatly suppressed, and the signal energy is concentrated within the specified bandwidth. The entire spectrum is cleaner, further verifying the excellent performance of the designed 8th-order Butterworth filter in extracting the target frequency band signal. At the same time, it also lays the foundation for subsequent envelope detection or demodulation.

4. CONCLUSION

This coursework systematically completed the entire process from DSB-SC modulation and synchronous demodulation, the realization of the superheterodyne receiver structure, to the analysis and processing of FM modulation signals.

In Q1 Part A, through upsampling of the Handel audio signal, DSB-SC modulation, synchronous demodulation and low-pass filtering, the original baseband signal was successfully restored, verifying the correctness of the DSB-SC-AM theory. In particular, multiplying the carrier signal by 2 during the modulation process effectively compensates for the amplitude loss and ensures the amplitude restoration of the modulated signal.

In Part B of Q1, the carrier extracted by the sawtooth wave through bandpass filtering was used for DSB-SC modulation, further consolidating the understanding of carrier generation, signal modulation and demodulation. Although the sawtooth wave itself has distortion, it can meet the modulation requirements after filtering optimization, and the recovered audio signal is clear, verifying the feasibility of actual carrier extraction.

In the Q2 section, by building a high-quality superheterodyne receiver link, the two frequency mixing and multi-level filtering of the signal are successfully achieved, effectively extracting the target baseband signal. The spectral variations at all levels are clear and in line with theoretical analysis. The system design is reasonable, and the final restored audio signal is clear and error-free, demonstrating the superiority of the superheterodyne structure in the reception of complex channels.

In the Q3 section, by analyzing the theoretical spectrum, actual generation and spectrum verification of the frequency modulation (FM) signal, the relationship between the Bessel function and the spectral energy distribution during the FM process was mastered. Meanwhile, for the FM signal after amplitude limitation, the spectral broadening phenomenon caused by nonlinear distortion was analyzed, and the target frequency band was successfully extracted through bandpass filtering, effectively restoring the modulated signal. The coursework deepened the understanding of frequency modulation characteristics, envelope extraction and spectrum processing.

In conclusion, this coursework not only verified various modulation and demodulation theories, but also enhanced the overall understanding of the functions and performance indicators of each module in the communication system through spectral analysis and time-domain processing, laying a solid foundation for the subsequent more in-depth design and optimization of the communication system.